Proceedings of the ASME 2020
International Design Engineering Technical Conferences and
Computers and Information in Engineering Conference
IDETC/CIE2021
August 17-20, 2021, Virtual, Online

DETC2021-XXXX

Automated Weld Path Generation Using Random Sample Consensus and Iterative Closest Point Workpiece Localization

Tristan Hill
Tennessee Technological University

Robert Shelton
Tennessee Technological **University**

Stephen Canfield
Tennessee Technological University

Fourth Author
Affiliation Here
Hyderabad, India

Fifth Author
Affiliation Here
Accra, Ghana

Sixth Author
Affiliation Here
Rome, Italy

ABSTRACT

Jobs performed by small to medium enterprises (SMEs) are infrequently automated due to high setup costs and lack of technical expertise needed for robot training, however productivity and worker safety can be improved in SMEs with the use automated tooling. In a traditional automated manufacturing environment, tasks such a welding or painting are accomplished through execution of pre-programmed tool motions which rely on the location and orientation of the workpiece to be fixed and known. The lack of this spatial information is typically treated through positioning of the workpiece with respect to the robot arm using jigs or fixtures which are costly in initial setup and not easily modified. Further, the resulting toolpath associated with a desired task is typically defined through manual teaching resulting in a path appropriate for an individual job. For this reason, SMEs requiring variation in part geometry or arrangement are not commonly automated. This work presents a method for automated weld path generation for a 6DOF co-bot arm using random sample consensus (RANSAC) and iterative closest point (ICP) workpiece localization from LiDAR pointclouds. Scans from a low cost 2D LiDAR mounted to the co-bot arm are used to generate 3D pointclouds of the workspace scene with the Robot Operating System (ROS). The Point Cloud Library (PCL) is used to compare the generated pointcloud with a CAD model to produce a rigid transformation to localize the workpiece. The estimated pose of the workpiece with respect to a fixed frame is used offline to generate a weld path as series of tool poses. Two example welding processes in which a cylinder or rectangular tube is joined to a flat plate and two square tubes are joined through weldment are investigated and a physical implementation of the method is demonstrated using a 2D LiDAR mounted to a 6DOF co-bot carrying a MIG welding torch.

Keywords: Place any keywords here

NOMENCLATURE

Place nomenclature section, if needed, here. Nomenclature should be given in a column, like this:

α	alpha
β	beta

1. INTRODUCTION

Small to medium enterprises perform manufacturing tasks associated with relatively low part volume and increased variation in assembly geometry as compared to jobs performed in large scale manufacturing environments. This type of manufacturing operation is infrequently automated due to high setup costs; however, productivity and worker safety can be improved in small to medium enterprises with the use of flexible automation such as automated tooling.

In a traditional automated manufacturing environment, a task such a welding or painting is accomplished through the execution of pre-programmed tool motions which rely on the location and orientation of the workpiece to be fixed and known with respect to a global coordinate system. The need for spatial information is typically treated through positioning of the workpiece with respect to the robot arm using jigs or fixtures which are costly in initial setup and are not easily modified. In large scale production environments, this can be accomplished with dedicated infrastructure built into the environment such as moving jigs on assembly lines and other features available in a highly structured environment. Further, the resulting toolpath associated with a desired task is typically defined through

manual teaching resulting in a path appropriate for an individual job. For this reason, SMEs requiring lower volume manufacturing with variation in part geometry or arrangement are not commonly automated.

As technology advances, humans and robots must adapt to remain relevant in our respective environments and this can currently be seen in the emergence of the co-bot workcell paradigm.

Presented in this paper is a method for automated weld path generation for a 6DOF co-bot arm using random sample consensus (RANSAC) and iterative closest point (ICP) workpiece localization implemented using the Robot Operating System (ROS) and the Point Cloud Library (PCL). Point Cloud Library provides an open-source C++ implementation of several 3D point cloud and image processing algorithms including: object recognition, filtering, feature estimation, surface reconstruction, registration, model fitting, and segmentation [5]. This library is an attractive research tool due to its stability, ability to integrate with ROS, and it includes example code and standard data sets that can be used for comparison repeatability in research.

This work employs a collection of these algorithms to locate, or register, a point cloud representing the workpiece in a point cloud of the working environment collected by a LiDAR scanner located on the robot. Once the known part is located with respect to a fixed frame, an automated weld path generation routine is used to plan a weld tool-path offline. Two example welding applications are presented. In the first, a square tube is joined to a flat plate through weldment. In the second, two square tubes are joined orthogonally to each other to form a tee. Simulations of both applications are investigated and a physical implementation of the method is demonstrated using a 2D LIDAR mounted to a 6DOF co-bot carrying a MIG welding torch which can be seen below in Figure 1.

Figure 1

Environment sensing devices which generate 3D points are frequently used in the mobile robotics industry, and improved sensors are being developed with the increased demand [5] for automation in manufacturing and transportation. A pointcloud is a list of points in 3D space representing a physical object or collection of objects [6][8], and this data is generated through measurements from a sensing device such as a LiDAR or 3D camera. Widespread applications and research involving spatial data has led to the development of standard file types, storage containers, and libraries for efficiently processing of pointclouds [5]. Common programming languages (C++, Python, MATLAB) support integration of pointcloud data with various libraries (PCL, OpenCV) and software frameworks (ROS).

The geometrical data, or features, stored in a pointcloud contain the locations of the boundaries of a solid object. Features may also include point normals which can be measured or inferred from the feature locations. Non-geometrical data such as color or other surface properties that are independent of the transformations between features are known as descriptors [13]. Descriptors are also used in feature based registration methods, which primarily depend on unique, descriptive features in order to obtain a match between pointclouds [6]. These two types of data contained in a pointcloud are stored separate because they are different in nature and are processed differently in algorithms such as segmentation or registration.

Figure 2 Method for Automated Weld Path Generation (NEEDS ARROWS!)

2. OVERVIEW OF APPROACH

The proposed approach to automated weld path generation shown in **Figure 1** consists of a model data preparation stage, a workspace sensing stage, a workpiece localization stage, followed by an offline robot path generation stage. The resulting path can be used to automate a welding process on the component in the workspace with a 6-DOF co-bot carrying a welding torch.

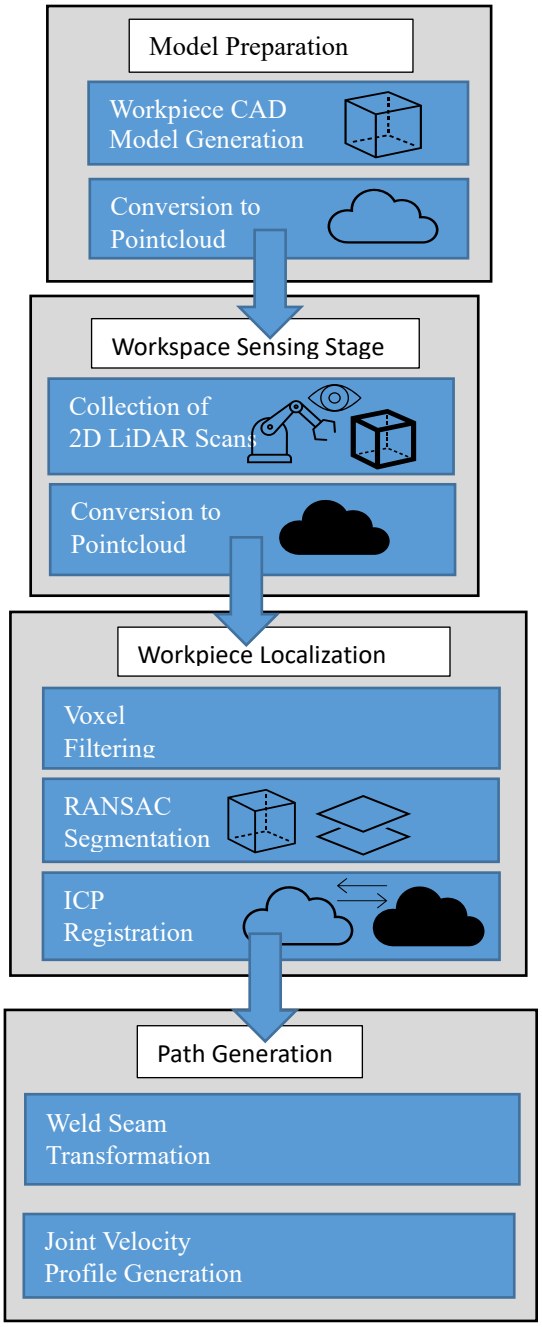

Figure 2

3. DESCRIPTION OF ALGORITHMS

Filtering w/ Bounding Box and Voxel
Segmentation w/ RANSAC
Correspondence Matching with ICP

4. MODEL PREPARATION STAGE

In the model data preparation stage, the geometry of the workspace and the workpiece is defined based on the prescribed application. An ideal model of the workpiece including the weldment is generated using CAD. Part models are first generated of the individual workpiece components which are then assembled to represent the workpiece. The CAD assembly representing the workpiece is converted into a pointcloud through a uniform sampling technique to be used for workpiece registration. The pointcloud associated with the CAD model is known as the source pointcloud.

A simplified model of the workspace and environment including the welding table and the robot base is also created for simulation purposes, and the environment model is also converted into a

pointcloud file. The 3D models are generated using standard CAD software from which they can be exported as .ply files or other standard file formats.

5. WORKSPACE SENSING STAGE

Prior to the sensing stage, the workpiece is placed in the robot workspace by the operator in the proper relative orientation to be joined by a weldment. The relative orientation of the parts must match that of the model to an extent and the global location of the workpieces is restricted to the usable workspace of the robot.

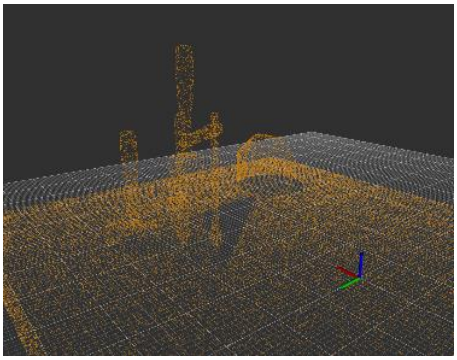

Fig 3a - Before Filtering

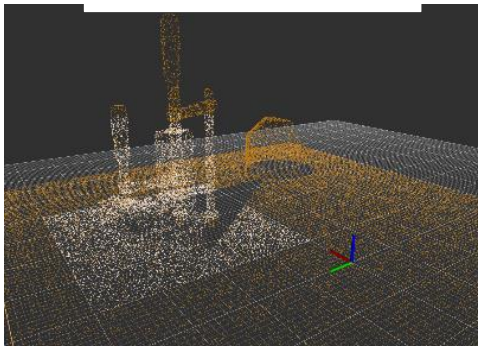

Fig 3b - After Voxel Filter

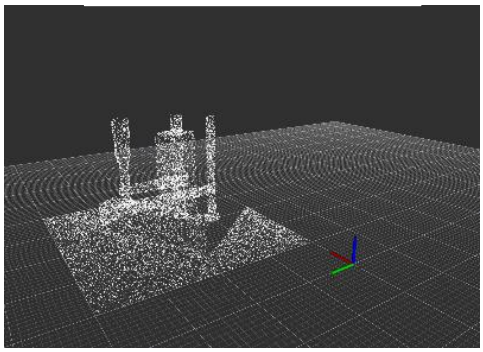

Fig 3c - After Bounding Box

Fig 3 - Filtering

In the sensing stage a sweeping motion of the arm is performed, and the workpiece and environment are scanned with the 2D LiDAR mounted on linkS of the robot. Multiple 2D lidar scans are measured along with corresponding sensor poses at (linkS). As the scanning stage continues, the data are transformed from the sensor frame linkS to the base frame link0 through the robot forward kinematics and accumulated into a 3D pointcloud with respect to the base frame. This process produces sparse data sets with redundant points. Therefore, the scans are filtered adownsampled (with methods within PCL) to improve results and reduce the resource requirements of storage and processing. The resulting pointcloud contains an image of the workpiece and fixtures as well as the top of the welding table and the background. The pointcloud associated with the LiDAR scan is known as the reference or target cloud. The sensing stage along with the methods of filtering and downsmpling can be seen below in figure 3.

6. WORKSPACE LOCALIZATION STAGE

In the workpiece localization stage, the **source pointcloud** derived from the CAD model is compared to the reduced **reference cloud** acquired from lidar in the sensing stage. The relative transformation between clouds is found using the iterative closest point algorithm (ICP). The pose of the two parts can be used to determine the required location of the weld seam in a global sense.

The reference cloud, collected from LiDAR, contains a larger volume of points, but not necessarily more points, than the source cloud. Also, the percentage of the workpiece represented in the LiDAR cloud depends on the sweeping motion used in the scanning stage and the amount of interference caused by the clamps or other obstructions. In the best-case scenario, approximately half of the points associated with the external faces of the workpiece are available in the LiDAR cloud.

The LiDAR cloud is first reduced to the usable workspace of the robot using a 3D bounding box removing points from the surrounding walls and extents of the table. Next, the point cloud is downsampled with a voxel filter [15] to ensure uniform density of points in the reference. The remaining image contains points from the workpiece, the clamps holding the workpiece, and the table. The robot arm may also be included in the remaining pointcloud. At this point, RANSAC based segmentation is used to compare geometrical information such as the planar nature of the table or the orthogonality of the workpiece to the LiDAR cloud to separate, or segment, the points associated with the workpiece. The results of a cascaded RANSAC segmentation are stored as the reference pointcloud cloud. Finally, the rigid transformation between the reference and source pointclouds is found with the iterative closest point (ICP) cloud registration algorithm. This transformation matrix represents the location and orientation of the workpiece with respect to a fixed origin.

7. SEGMENTATION WITH RANSAC

One of the key issues with standard ICP is that it may not reach the global minimum of convergence which can be due to things such as false correspondences. These false correspondences cause poor initial alignment and therefore increase the chance of getting stuck in a local minimum [7]. Outlier rejection based on Random Sample Consensus (RANSAC) is one of the several methods including distance-based rejection, or duplicate target point rejection, that reduces the number of outliers in pointclouds. Furthermore, RANSAC may also be utilized to provide a good initial guess for the transformation estimation in ICP [6]. The RANSAC algorithm, in general, is a resampling technique that uses the minimum number of data points required to correctly detect and segment pointcloud shapes [10][11].

Although variations have been developed, the RANSAC algorithm can generally be thought of as an iterative two-part process. The first part involves a hypothesis in which the first minimal sample set (MSSs) is selected at random from the input dataset (source pointcloud) which is then used as the basis for computing the model parameters. Following the selection of the minimal sample set, RANSAC checks which elements of the instantiated model are consistent with the entire dataset – these elements are referred to as the consensus set (CS) [10]. During each iteration, the instantiated model's elements are comparted to the original dataset. If the new MSS increases the number of correct correspondences compared to the best CS, it will then overwrite the previous CS. The algorithm continuously iterates and is terminated only when the CS reaches a certain threshold. When this threshold has been reached, the instantiated model based on model parameters of the newest MSS, the MSS is said to be consistent with the entire dataset.

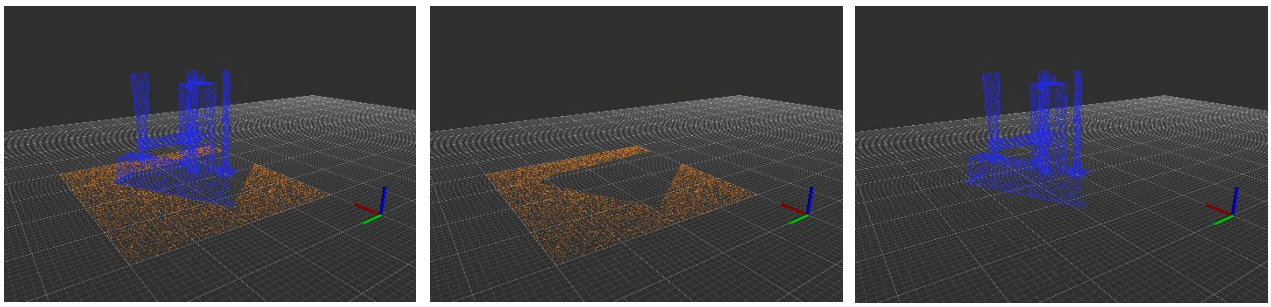

Figure 4a – Input Cloud: Table, Workpiece, and Clamps

Figure 4b – Plane Inliers: Table

Figure 4c – Plane Outliers: Workpiece and Clamps

Figure 4 – Segmentation to Remove Table

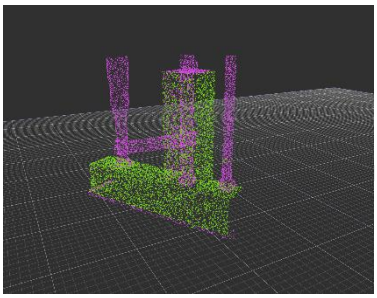

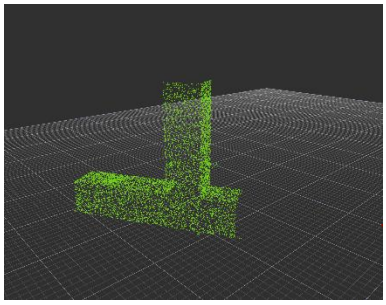

Figure 4b – Plane Inliers: Workpiece

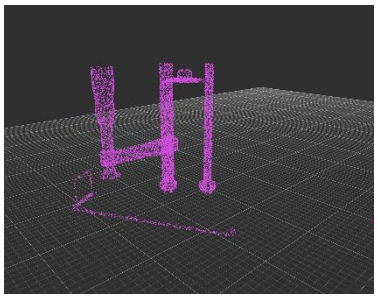

Figure 4c – Plane Outliers: Clamps

Figure 5 – Segmentation to Remove Clamps

8. ITERATIVE CLOSEST POINT

The objective of the original ICP algorithm is to find a rigid transformation, with which the reference cloud is in the best alignment with the source pointcloud set. This method considers the closest corresponding points between two pointclouds and estimates a transformation to minimize the distance between them using a method of least squares [6]. By iteratively registering the reference cloud with the source cloud and applying rotation matrix R and a translation vector *t,* the source point set is expected to converge as the correspondences achieve alignment. This method however, has also been proven to be locally convergent, which means that the algorithm easily fails when the rotation angle between two point-sets is large [7]. For this reason, a good initial transformation is important such that it guarantees that the algorithm converges to the global minimum [7]. In this work, false correspondences from the environment scans are known to inhibit convergence. An implementation to reduce these false correspondences, such as RANSAC, is included.

The primary challenge in the localization stage is the selection of point clouds to use as inputs to the ICP algorithm [4],[7]. It has been shown and verified in this work that the success of the alignment process is highly dependent on the correspondence between input data sets. The existence of points in one cloud which are not represented in the other cloud can only add cost [6] to the alignment process. Further, significant amounts of outliers will cause the alignment to fail or perform poorly. Modifications to ICP and alternative algorithms have shown improved performance [4] [6] in the presence of outliers, and methods are available (used in this approach) for automatic rejection of non-corresponding outliers (in let rev?). However, the approach in this work addresses the problem by reducing the reference point cloud to a subset of the LiDAR cloud which contains a portion of the workpiece without the surrounding table or clamps.

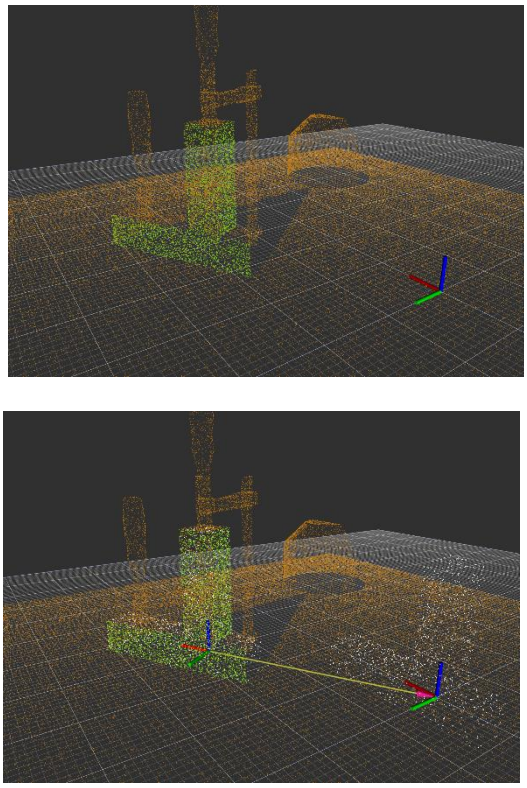

Figure 6 – Workpiece Localization with ICP

9. CORRESPONDENCE MATCHING AND ALIGNMENT (ICP)

The ICP method as described in [12] is summarized here. Let $R_P = \{\vec{r}_i\}$ be the reference point cloud set for $i = 1,2,\dots,N_P$

representing the workpiece to be aligned with the source point cloud set $S = \{\vec{s}_k\}$ for $k = 1,2,\dots,N_S$ where $N_i = N_k$, and where each point $\vec{r}_i$ corresponds to the point $\vec{s}_k$ with the same index (i=k). The reference set R_P will come from a CAD model while the source cloud set S will be collected from a data scan of the real environment. The mean square objective function (Point-to-Point Error Metric) to be minimized is,

$$E(R,t) = \frac{1}{N_s}\sum_{i=1}^{N_S}\|r_i - Rs_i - t\|^2. \quad (1)$$

where $R \in \mathbb{R}^{3x3}$ is an $so(3)$ array that projects S onto R_P and $t \in \mathbb{R}^3$ that translates S onto R_P. If the correct correspondences are known, the correct relative rotation/translation can be calculated in closed form. A closed form implementation that can be found in the PCL library (cite) is briefly described. The center of mass μ_{R_p}, μ_S for the reference point cloud set and source point cloud set respectively is calculated for each set as,

$$\mu_{R_p} = \frac{1}{N_r}\sum_{i=1}^{N_r} r_i \quad \text{and} \quad \mu_S = \frac{1}{N_s}\sum_{i=1}^{N_s} s_i. \quad (2)$$

The reference point cloud set and source point cloud set are shifted by their center mass such that they are distributed around zero as,

$$R_p{}' = \{r_i - \mu_r\} = \{r_i'\} \quad (3)$$

$$S' = \{s_i - \mu_s\} = \{s_i'\}$$

A cross-covariance matrix, $W \in \mathbb{R}^{3x3}$ is defined as

$$W = \sum_{i=1}^{N_r} r_i' s_i'^T. \quad (4)$$

A singular value decomposition (SVD) of W is given as

$$W = UDV^T \quad (5)$$

where D is a diagonal matrix containing the singular values, $\sigma_i, i = 1{:}\,3$, ordered such that $\sigma_1 \geq \sigma_2 \geq \sigma_3$ and $U \in R^{3x3}$, $V \in R^{3x3}$ are the left and right singular vectors of W. When the $rank(W) = 3$, the rotation R and translation t minimizing $E(R,t)$ are unique and given by:

$$R = UV^T \quad (6)$$

and

$$t = \mu_r - R\mu_s \quad (7)$$

In practice, the correspondences assumed in Eq. (1) are not truly known. Therefore, this process is performed iteratively, by assuming a correspondence between the reference and source point cloud set based on a minimum distance between points. The source is corrected and the process repeats until convergence of the source and reference point cloud set occurs as given in the error $E(R,t)$.

10. PATH GENERATION STAGE

Transformation of Seam Points

Consider a pointcloud set $R_{Seam} = \{\vec{r}_k\}$ for $k = 1,2,\dots,N_S$ located along the weld seam as described by the example application and defined in the CAD model. The weld seam exists at the shared location of the connecting faces of the two parts which make up the workpiece. The pointcloud set R_{Seam} is a subset of the pointcloud set R_{Part} which represents the workpiece.

$$R_{Seam} \subseteq R_{Part}$$

The pointcloud set R_{Seam} and R_{Part} are defined with respect to a frame {{part}} located on the workpiece.

To complete the desired operation the robot must carry the torch along the weld seam. The path generation stage requires the robot tool path points to be described with respect to the fixed frame of the robot. The pointcloud sets R_{Seam} and R_{Part} can be projected into the fixed frame of the robot with the rigid transformation for T_{Robot}^{Part} resulting from the ICP routine described previously as it is the best available approximation of the workpiece pose.

The set of points $R_{Tool} = \{\vec{r}_l\}$ for $l = 1,2,\dots,N_T$ is found by applying the rotation R and translation t separately as shown. T_{Robot}^{Part} = fn(R, t)

$$R_{Tool} = \{Rr_k + t\} \text{ for } k = 1,2,\dots,N_S$$

Joint Velocity Profile Generation

11. IMPLEMENTATION USING ROS AND PCL

This research has been implemented in ROS on Ubuntu Linux which provides a multi-threaded and distributed software framework for robotics applications.

The combination of 2D LiDAR scans into 3D pointclouds was done using a custom ROS package *scan2cloud* that is based on *ROS laser_geometry*. The rigid transformation from the sensor frame to the base of the robot is programmed with *ROS tf* so that individual 2D scans collected using *ROS rplidar* can be processed and saved as a .pcd file with respect to a global origin.

The .pcd file is used for permanent storage and several pointcloud data types

The robot and sensor are operated simultaneously using ROS, and the resulting pointcloud is saved as a .pcd file which can be processed using the Point Cloud Library or converted to a .ply polygon file.

12. MANUFACTURING APPLICATION

A manufacturing task is considered, in which a weldment is performed on a workpiece resting on a welding table. The workpiece in this task consists of multiple components to be joined through weldment. The relative alignment of the multiple components of the workpiece is assumed to be correct within the physical constraints of the designed part prior to the automated process. In practice, this alignment is set by the operator and secured using clamps or other fixtures.

Variation in surface quality and workpiece dimension and shape are likely present however these are not the focus of this process. The workpiece geometries are generally assumed to match those in the model within a working tolerance. These local model

inaccuracies certainly affect the global information produced regarding the geometry and location of the weld, but these affects are minor.

Two example applications are considered. In the first of which, two square tubes are joined perpendicular to one another with a fillet weld along two of the shared edges. In the second application, a square tube is joined to a flat plate with a fillet weld along the shared edge between the two components. In each of these examples, the assembly is temporarily joined together by clamps which will be included in the lidar scan. Prior to the alignment process, these clamps will be removed from the pointcloud data via segmentation with RANSAC.

In example application 1 the workpiece consists of two square tubes to be joined by weldment so that the tubes are perpendicular and form a tee.

In example application 2 the workpiece consists of a square tube to be joined by weldment to a flat plate so that the tube is perpendicular to the plate.

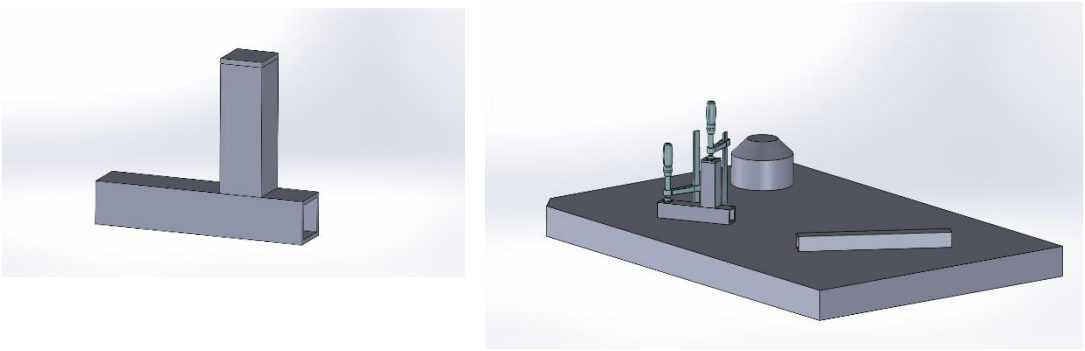

Figure 7 – Example Application A

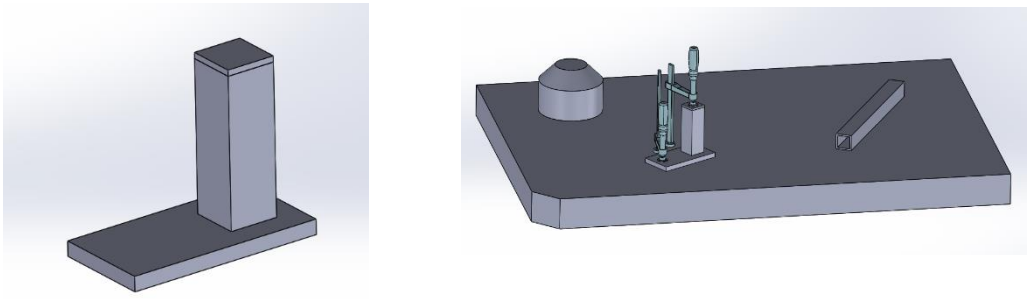

Figure 8 – Example Application B

13. SIMULATION RESULTS

Example application A and B were performed for testing and validation of the proposed approach using synthetic data generated from CAD models of the workspace including the table and clamps as shown in the figure above. The models of the scene were converted to pointclouds using the uniform sampling process described for the conversion of the source cloud.

14. EXPERIMENTAL RESULTS

Example Application A was performed with an Aubo i5 on a welding table with a RP-LiDAR A2 mounted to the end effector for generating 3D pointsclouds. In the scanning stage the arm performed a sweeping motion while collecting a point cloud containing approximately half of the workpiece, a large portion of the table, and a small portion of the arm itself. The recorded points are restricted to those that fall in a selected region of the usable workspace of the robot. This collection process produces redundant data points representing the objects and the cloud data can become large. The approach presented is applied to the raw projected LiDAR points as described with respect to the base frame of the robot.

Experimental Calibration

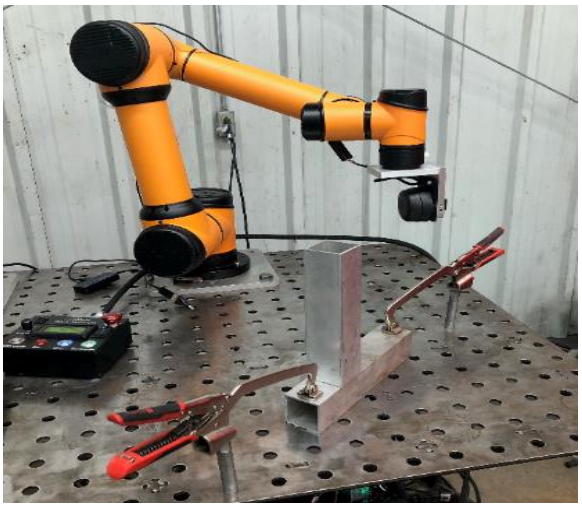

Figure - Experimental Setup for Application A

Type equation here.

2.1 Subtitle

Subtitles should be bold but not all-capped.

15. RESULTS AND DISCUSSION

3D Lidar Calibration

	X (m)	Y (m)	Z (m)		
Expected Translation	0.0	-0.60960	0.02540		
Measured Translation	0.00893	-0.60874	0.02003		
Difference	-0.00893	-0.00086	0.00537		

	X (m)	Y (m)	Z (m)		
Expected Translation	0.10160	-0.60960	0.02540		
Measured Translation	0.10840	-0.61096	0.02034		
Difference	-0.00680	0.00136	0.00506		

Simulated Application A

	Roll (rad)	Pitch (rad)	Yaw (rad)		
Expected Rotation	0.0	0.0	0.0		
Measured Rotation	-0.00493	-0.00071	0.019938		
Difference	0.00493	0.00071	-0.00071		

	Roll (rad)	Pitch (rad)	Yaw (rad)		
Expected Rotation	0.0	0.0	0.785		
Measured Rotation	-0.00457	0.02186	0.79461		
Difference	0.00457	-0.02186	-0.00921293		

Example Application A

	X	Y	Z		
Expected Translation	0.25	0.2	0.025		
Measured Translation	0.251347	0.19923	0.02436		
Difference	-0.00134	0.00077	0.00064		

	Roll	Pitch	Yaw		
Expected Rotation	0.0	0.0	0.52360		
Measured Rotation	-0.00918	-0.00681	0.52759		
Difference	0.00918	0.00680	,-0.00399		

Results and Conclusion

The results show that the proposed method of automated weld path generation effectively using RANSAC and ICP algorithms is viable for workpiece localization. The alignment achieved in the simulated examples is strong as shown in the table and proved that these algorithms can be implemented even in the case of increased noise in the target point cloud due to clamping mechanisms or miscellaneous items on the weld surface. The accuracy of the simulated tests is to be expected given that the simulated scene contained geometric features designed in CAD which closely resembled the target pointcloud features.

The physical experiment shows that this approach can be applied to a welding application using physical data in a realistic environment given that proper calibration is completed. The 3D LiDAR scans require calibration to accurately transform the source cloud to the target cloud. Further investigation is required to determine if the accuracy of the resulting workpiece localization is inside a working tolerance for a welding operation.

The implementation of down sampling and filtering with voxel and bounding box is an essential step prior to the segmentation algorithm with RANSAC. Furthermore, with the increased utilization of RANSAC, outlier rejection is a required step when there are features such as clamps included in the target pointlcoud set. Correspondence matching and alignment with ICP is proven to only be effective when sufficient outliers have been rejected and a good initial guess is provided by RANSAC. Utilization of cascaded RANSAC segmentation provides an effective means for sufficient outlier removal such that workpiece alignment accurate enough to be applied to a physical welding process.

Place any acknowledgements here.

REFERENCES

Bibliography

[1] Segal, A. V., Haehnel, D., and Thrun, S., 2010, “Generalized-ICP,” Robotics: Science and Systems.
[2] Fischler, M. A., and Bolles, R. C., 1981, “Random Sample Consensus: A Paradigm for Model Fitting With,” Commun. ACM.
[4] Zhang, J., Yao, Y., & Deng, B. (2021). Fast and Robust Iterative Closest Point. IEEE Transactions on Pattern Analysis and Machine Intelligence.
[5] Rusu, R. B., and Cousins, S., 2011, “3D Is Here: Point Cloud Library (PCL),” Proceedings - IEEE International Conference on Robotics and Automation.
[6] Zhao, H., Anwer, N., et. Al., 2016, “Registration with the Point Cloud Library PCL,” IEEE Int. Conf. Intell. Robot. Syst.
[7] Du, S., Xu, Y., Wan, T., Hu, H., Zhang, S., Xu, G., and Zhang, X., 2017, “Robust Iterative Closest Point Algorithm Based on Global Reference Point for Rotation Invariant Registration,” PLoS One.
[8] Schwarz, S., Preda, M., Baroncini, V., Budagavi, M., Cesar, P., Chou, P. A., Cohen, R. A., Krivokuca, M., Lasserre, S., Li, Z., Llach, J., Mammou, K., Mekuria, R., Nakagami, O., Siahaan, E., Tabatabai, A., Tourapis, A. M., and Zakharchenko, V., 2019, “Emerging MPEG Standards for Point Cloud Compression,” IEEE J. Emerg. Sel. Top. Circuits Syst.
[9] Galin, R., Meshcheryakov, R., Kamesheva, S., and Samoshina, A., 2020, “Cobots and the Benefits of Their Implementation in Intelligent Manufacturing,” *IOP Conference Series: Materials Science and Engineering*.
[10] Zuliani, M., 2008, “RANSAC for Dummies,” Citeseer.

[11] Li, L., Yang, F., Zhu, H., Li, D., Li, Y., and Tang, L., 2017, “An Improved RANSAC for 3D Point Cloud Plane Segmentation Based on Normal Distribution Transformation Cells,” Remote Sens.
[12] Besl, P. J., and McKay, N. D., 1992, “A Method for Registration of 3-D Shapes,” IEEE Trans. Pattern Anal. Mach. Intell.
[13] Wang, F., Liang, C., Ru, C., and Cheng, H., 2019, “An Improved Point Cloud Descriptor for Vision Based Robotic Grasping System,” Sensors (Switzerland).
[14] Moreno, C., and Li, M., 2016, “A Comparative Study of Filtering Methods for Point Clouds in Real-Time Video Streaming,” *Lecture Notes in Engineering and Computer Science*.
[15] Zygmunt, M., 2013, “The Testing of PCL: An Open-Source Library for Point Cloud Processing,” Geomatics, Landmanagement Landsc.